Diagnostic Accuracy Study

Medicine®

OPEN

Computed tomography pulmonary angiograms using a novel dual-layer spectral detector

Adjusted window settings are essential for diagnostic image quality

Andra-Iza Iuga[a,*], Jonas Doerner, MD[a], Florian Siedek, MD[a], Stefan Haneder, MD[a], Jonathan Byrtus, MD[a], Julian A. Luetkens, MD[b], David Maintz, MD[a], Tilman Hickethier, MD[a]

Abstract

Objective: The aim of this study was to determine optimal window settings for conventional polyenergetic and virtual monoenergetic images derived from computed tomography pulmonary angiogram (CTPA) examinations of a novel dual-layer spectral detector computed tomography system (DLCT).

Methods: Monoenergetic (40 keV) and polyenergetic images of 50 CTPA examinations were calculated and the best individual window width and level (W/L) values were manually assessed. Optimized values were obtained afterwards based on regression analysis. Diameters of standardized pulmonary artery segments and subjective image quality parameters were evaluated and compared.

Results: Attenuation and contrast-to-noise values were higher in monoenergetic than in polyenergetic images ($P \leq .001$). Averaged best individual W/L for polyenergetic and monoenergetic were 1020/170 and 2070/480 HU, respectively.

All adjusted W/L-settings varied significantly compared to standard settings (700/100 HU) and obtained higher subjective image quality scores. A systematic overestimation of artery diameters for standard window settings in monoenergetic images was observed.

Conclusions: Appropriate W/L-settings are required to assess polyenergetic and monoenergetic CTPA images of a novel DLCT. W/L-settings of 1020/170 HU and 2070/480 HU were found to be the best averaged values for polyenergetic and monoenergetic CTPA images, respectively.

Abbreviations: Avg. = averaged, Calc. = calculated, CNR = contrast-to-noise ratio, CTPA = computed tomography pulmonary angiogram, DECT = dual-energy computed tomography, DLCT = dual-layer spectral detector computed tomography, DSCT = dual-source spectral detector computed tomography, HU = Hounsfield Units, Ind. = individual, L = level, MonoE = virtual monoenergetic imaging, PolyE = polyenergetic imaging, ROI = region of interest, SD = standard deviation, SNR = signal-to-noise ratio, Std. = standard, W/L = width and level settings, W = width.

Keywords: dual-energy CT, pulmonary angiography, spectral detector CT, virtual monoenergetic imaging, window settings

1. Introduction

Virtual monoenergetic images (MonoE) calculated from dual-energy computed tomography (DECT) raw data have become increasingly popular as they are considered to provide certain benefits compared to conventional polyenergetic images (PolyE) in a wide range of indications such as oncological staging scans, vascular examinations, or neuroimaging.[1–7]

High- and low-energy datasets of the polyenergetic x-ray spectra are needed to calculate these MonoE. To obtain these 2 x-ray datasets, various solutions are available. Currently, they can be generated at the output of the x-ray tube by 2 independent tube-detector systems at different tube potentials (dual-source), 2 consecutive rotations of a single x-ray source at different tube potentials (dual-spin), rapidly switching the tube potentials of a single x-ray source during a single rotation (kVp switching), or using a beam filter to split the output of a single x-ray source, resulting in 2 partial beams with high and low mean energies (split or twin beam).[8]

However, recently a detector-based solution became available. This technique uses a single x-ray source with a dual-layer detector which registers the low-energy photons in a superficial yttrium-based layer, whereas the higher-energy electrons are detected in a subjacent gadolinium-oxysulfide-based layer.[9]

Although x-ray-tube-based DECT systems only allows dual-energy post-processing in the image data space (or need preceding temporal and angular interpolation), the dual-layer spectral detector computed tomography system (DLCT) enables direct spectral post-processing of the raw data. This is feasible because

Editor: Robert Chen.

The authors report no conflicts of interest.

[a] Institute of Diagnostic and Interventional Radiology, Faculty of Medicine and University Hospital Cologne, University of Cologne, Cologne, [b] Institute of Diagnostic and Interventional Radiology, University of Bonn, Bonn, Germany.

[*] Correspondence: Andra-Iza Iuga, University Hospital of Cologne, Kerpener Str. 62, 50937 Köln, Germany (e-mail: andra.iuga@uk-koeln.de).

Medicine (2019) 98:33(e16606)

Received: 12 February 2019 / Received in final form: 1 July 2019 / Accepted: 3 July 2019

http://dx.doi.org/10.1097/MD.0000000000016606

of the simultaneous measurement of the low- and high-energy data in consistent spatial and angular location[10] and is essential for a significant reduction in image noise.[11] This novel method is particularly valuable for monoenergetic reconstruction at low-energy levels (low keV MonoE), which are prone to elevated noise levels in tube-based DECT[12] and also potentially provides the best contrast- (CNR) and signal-to-noise ratios (SNR) in contrast-enhanced scans owing to the approximation to the iodine k-edge at 33 keV.[13–15]

This strong increase in iodine attenuation is likely to be advantageous for the evaluation of vessels containing iodinated contrast agents. However, to exploit this advantage and obtain an optimized readability of low keV MonoE, individual adjustments of the display window settings (window width and level in HU [W/L]) are essential.[16,17]

In the last several years, such optimized window setting protocols were introduced for arterial and portal-venous phase imaging of the abdomen for DECT systems using a dual-source approach.[17–21] Regarding optimized settings for computed tomography pulmonary angiograms (CTPA), there is currently only 1 study available that used a x-ray tube-based DECT system, namely a dual-source computed tomography system (DSCT).[22] For DLCT examinations, however, no data exist yet.

Therefore, the aim of this study was to determine the most appropriate W/L settings for conventional polyenergetic and low keV MonoE for CTPA examinations of a novel DLCT system for the evaluation of pulmonary arteries. As previous studies found distal vessel branches to be especially challenging to assess,[23] they were used as a particular assessment focus in our present study.

2. Materials and methods

2.1. Study population

Ethical approval was waived because of the retrospective design of the study based on preexisting examinations. The study population comprised of 50 patients (25 males; mean age 60 ± 17.5 years) who were referred to CTPA upon suspicion of pulmonary embolism from June 2016 to January 2017.

2.2. Image acquisition and post-processing

All examinations were conducted with a 128-slice DLCT-system (IQon, Philips Healthcare, Best, The Netherlands). Patients were scanned in a supine craniocaudal direction during inspiration breath-hold. The clinical routine protocol used in this study included pulmonary angiographic phase imaging of the chest obtained after a bolus injection of 60 mL nonionic, iodinated contrast agent (Accupaque 350 mg/mL, GE Healthcare; Little Chalfont, UK) via an antecubital vein at a flow rate of 4 mL/s followed by a 30-mL saline chaser. For contrast timing, a bolus-tracking technique was used in all cases which automatically started the examination with a 5-second scan delay after a trigger threshold of 150 HU had been reached within a circular region of interest (ROI) placed within the pulmonary trunk. The following scanning parameters were kept constant in all scans: collimation $2 \times 64 \times 0.625$ mm; rotation time, 0.33 seconds; pitch, 1.171; tube current, 120 kVp; matrix 512×512; dose modulation type: DoseRight 3D-DOM (Philips Healthcare, Best, The Netherlands). All axial images were reconstructed with a slice thickness of 2 mm and a section increment of 1 mm using a dedicated spectral reconstruction algorithm with a strength level of 3 (comparable to conventional hybrid iterative reconstructions methods, eg, Philips iDose[4]) and a constant kernel (Spectral B; Philips Healthcare, Best, The Netherlands). In addition to the conventional 120 kV PolyE images, MonoE images were reconstructed at 40 keV. Imaging analysis was performed offline on a dedicated workstation (IntelliSpace Portal 6.5, Philips Healthcare, Best, The Netherlands).

2.3. Quantitative and Qualitative Image Analysis

Every image dataset was assessed by 2 radiologists, each with 5 years of experience in CT imaging. Circular ROIs were placed in the pulmonary artery (at the level of its bifurcation), the infraspinatus muscle, the subcutaneous fat, and the surrounding air. Attenuation values (in Hounsfield Units) and standard deviations (SD) were averaged and compared between reconstructions.

Image noise was defined as SD of attenuation of the subcutaneous fat. Contrast-to-noise ratio (CNR) was calculated for each dataset using the following equation: $(HU_{pulmonaryartery} - HU_{muscle})/SD_{fat}$.

Two same readers independently evaluated all reconstructions randomly in a blinded manner. Each reader manually measured the cross diameter of the left anterior segmental artery (5 cm distal of its origin from the left main pulmonary artery) to assess the influence of W/L settings on vessel sizing. Measurements were performed twice and averaged.

Subjective image quality was rated for all reconstructions and all window settings (standard [Std. W/L, individual [Ind.]-W/L, calculated [Calc.]-W/L, average [Avg.]-W/L) based on vessel delineation and on image noise using a 4-point Likert scale (1 = poor vessel delineation/high image noise; 2 = moderate/moderate; 3 = good/low; 4 = excellent/insignificant) for the pulmonary artery tree, with special focus on distal vessel branches.

As previously mentioned, these predefined distal vessel branches were used as a primary assessment focus in this study. However, towing to their small size, for quantitative measurements different measuring locations had to be used (as listed above). They were selected because of the following reasons: to allow well-dimensioned and therefore reliable ROI measurements of pulmonary artery attenuation, these measurements were obtained at its maximum diameter, the pulmonary artery bifurcation. The measurements of the artery cross diameters were taken of the left anterior segmental artery because of its consistent anatomy and appropriate size.

2.4. Window settings

Image datasets were separately evaluated on a dedicated workstation (IntelliSpace Portal 6.5, Philips Healthcare, Best, The Netherlands). Interpretation bias was avoided by evaluating the datasets in a random order. Also, both readers were unaware of the applied reconstruction method. Both readers independently chose their preferred window settings for pulmonary artery-focused assessments in MonoE as well as PolyE reconstructions by manually adjusting the W/L settings in every reconstruction to achieve the most suitable W/L combination. As previously mentioned, W/L settings were optimized with regard to the assessment of the distal branches of the pulmonary artery (the left segment 1 segmental artery and its distal branches was predefined as common assessment focus). These W and L values were

recorded, separately averaged between the readers and referred to as "best individual" values (Ind.-W/L) for every patient.

Afterwards, linear regression analysis between the Ind.-W/L and the absolute attenuation values of the pulmonary artery was performed. For each reconstruction, HU values of the pulmonary artery were plotted against the Ind.-W/L window parameters resulting in 2 scatterplots for each reconstruction (1 for width and 1 for level). A line was fitted through these scatterplots with its origin forced through zero to obtain linear regression equations for each parameter and reconstruction type.

Then, "calculated individual" width and level settings (Calc.-W/L) were computed for each reconstruction by using these equations and "averaged mean" width and level settings (Avg.-W/L) were obtained by averaging all Calc.-W/L values for each reconstruction type.

Common accepted standard window settings (Std.-W/L) for pulmonary artery assessment in general (unchanged from CT scanner defaults and without specific focus; W/L 700/100 HU[24,25]) were used for comparison.

2.5. Statistical analysis

GraphPad Prism (version 7.0b for Macintosh, GraphPad Software, La Jolla, CA) was used for the statistical analysis. Descriptive statistics are summarized as means ± SD. All data were tested for normality using the D'Agostino-Pearson omnibus K2 test. Parametric data (windows settings and quantitative image parameters) were analyzed using paired *t* tests or repeated measures analysis of variance followed by Tukey's multiple comparisons post-hoc test (depending on the number of comparisons). Nonparametric data (subjective image quality scores and differences between both readers) were analyzed using Wilcoxon or Friedman test (depending on the number of comparisons). Statistical significance was defined as $P \leq .05$.

3. Results

3.1. Attenuation analysis

Mean attenuation of the pulmonary artery was 326.0 ± 96.7 HU in PolyE reconstructions and 1111.0 ± 373.4 HU in MonoE at 40 keV. Image noise was slightly (yet significantly) lower in MonoE (21.9 ± 6.4 HU) compared to PolyE images (25.6 ± 7.3 HU; $P < .001$). Resulting CNRs were significantly higher at MonoE 40 keV images compared to PolyE reconstructions (53.6 ± 23.8 vs 12.1 ± 5.7 HU). All quantitative results are summarized in Table 1.

3.2. Window settings:

For PolyE images, averaging of all Ind.-W/L values resulted in W values of 1034 ± 485 HU and L values of 183 ± 57 HU. Averaged W and L values for MonoE 40 keV reconstructions were 2122 ± 650 HU and 402 ± 270 HU. Equations of optimized W and L were derived for each reconstruction type from regression analyses of absolute attenuation of the pulmonary artery and the individual Ind.-W/L values.

Equations were as follows:

Calculated W for PolyE: 3.297 × HU
Calculated L for PolyE: 0.5472 × HU
Calculated W for 40 keV: 1.948 × HU
Calculated L for 40 keV: 0.4517 × HU

Table 1

Quantitative results.

	PolyE	MonoE	*P* PolyE vs MonoE
Attenuation pulmonary artery, HU	326.0 ± 96.7	1111.0 ± 373.4	**<.001**
SD fat, HU	25.6 ± 7.3	21.9 ± 6.4	**<.001**
CNR pulmonary artery, HU	12.1 ± 5.7	53.6 ± 23.8	**<.001**

Note: significant differences are shown in bold. Values expressed as mean ± SD. CNR = contrast to noise ratio, MonoE = virtual monoenergetic imaging at 40 keV, PolyE = polyenergetic imaging, SD = standard deviation.

Calc.-W/L values were then calculated for each individual examination and reconstruction. When averaged, this resulted in a mean W and L for PolyE imaging of 1022 ± 319 and 168 ± 53 HU, of which Avg.-W/L values of 1020/170 were rounded. For MonoE 40 keV reconstructions, mean Calc.-W/L of 2069 ± 727 and 480 ± 168 HU were calculated, which were rounded to Avg.-W/L values of 2070/480 HU. Figure 1 shows a representative image data set with the different W/L settings.

No significant differences were observed between Ind.-W/L and Calc.-W/L for both, W and L in both reconstruction types. In contrast, significant differences were found for both reconstruction types between Std.-W/L and Ind.- W/L for both, W and L (all $P < .001$). Additionally, Ind.-W/L and Calc.-W/L were significantly higher for MonoE than for PolyE (all $P < .001$). Table 2 presents a complete statistical analysis.

3.3. Subjective Analysis

All assessed subjective image quality parameters were substantially impaired in standard window setting of 700/100 HU in comparison to the corresponding Ind.-W/L. For both, vessel delineation and image noise, there were no significant differences between manually adjusted (Ind.), mathematically calculated individual (Calc.) or averaged adjusted window settings (Avg.) in both reconstruction types. However, Ind.- W/L tended to obtain highest scores (Table 3).

There was no significant difference in between the subjective results of both readers' scores. Complete comparison of subjective ratings is shown in Table 4.

3.4. Objective analysis

No significant differences were observed in measured left segment 1 pulmonary artery diameters for PolyE reconstructions among all window settings (all $P > .05$; Table 5 gives a summary of the comparisons). For MonoE, a systematic overestimation of vessel diameters was shown for standard window settings compared to the individual adjusted window settings (all $P < .001$; see Table 5). Additionally, manually optimized window settings for MonoE 40 keV reconstructions revealed slightly smaller diameters than PolyE images (all $P < .001$; see Table 5).

4. Discussion

The purpose of this study was to determine optimal window settings for pulmonary angiogram CT examinations of a novel DLCT for conventional polyenergetic and virtual MonoEs at 40 keV. Both examinations, with and without pulmonal emboli were included, but the analysis was focused on optimal vessel delineation, not on thrombus detection. The different

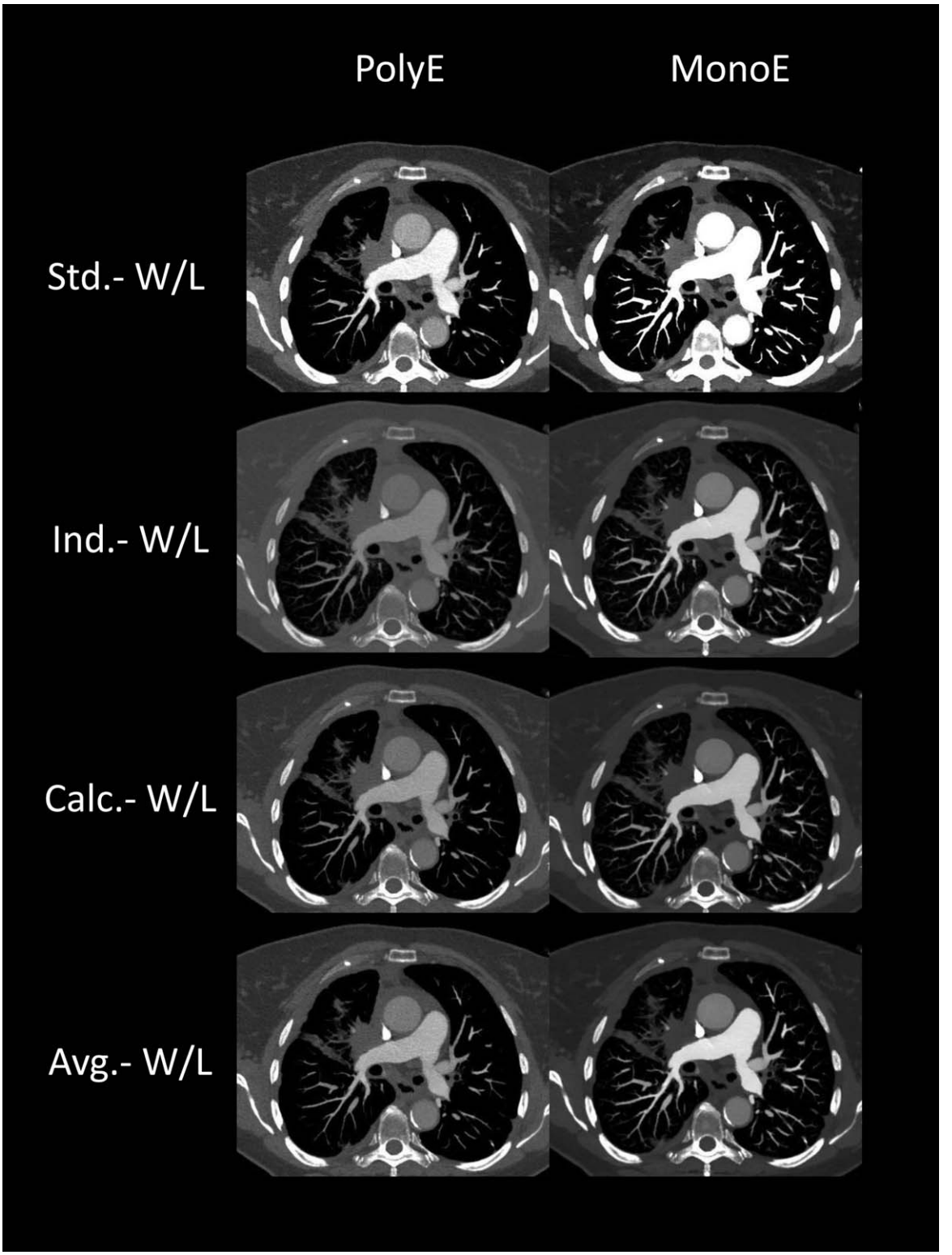

Figure 1. Complete image dataset showing PolyE and MonoE 40 keV images with the 4 different window settings for pulmonary artery assessment. Note the excessive overexposure if standard window settings were used for MonoE images, which led to an overestimation of vessel size. With adjusted window settings, artery assessability (particularly of the distal branches) was considerably improved. Ind.-W/L = individual width and level settings, MonoE = virtual monoenergetic imaging at 40 keV, PolyE = polyenergetic imaging, Std.-W/L = standard width and level settings.

measurements were conducted at the most suitable location for each measurement. In theory, results in different parts of the pulmonary artery tree could vary, but clinically this influence is likely to be negligible and the probability that unreliable measurement owing to inappropriate measurement locations would distort the results was considerably higher.

Table 2

Window settings.

Pulmonary artery					
	Mean width, HU	**Mean level, HU**	**Comparison**	**Width**	**Level**
Std.-W/L	700	100	Std-W/L vs Ind.-W/L PolyE	**<.001**	**<.001**
Ind.-W/L PolyE	1034 ± 485	183 ± 57	Ind.-W/L PolyE vs Calc.-W/L PolyE	.95	.89
Calc.-W/L PolyE	1022 ± 319	168 ± 53	Std-W/L vs Ind.-W/L MonoE	**<.001**	**<.001**
Avg.-W/L PolyE	1020	170	Ind.-W/L MonoE vs Calc.-W/L MonoE	.97	.93
Ind.-W/L MonoE	2122 ± 650	402 ± 270	Ind.-W/L PolyE vs Ind.-W/L MonoE	**<.001**	**<.001**
Calc.-W/L MonoE	2069 ± 727	480 ± 168	Calc.-W/L PolyE vs Calc.-W/L MonoE	**<.001**	**<.001**
Avg.-W/L MonoE	2070	480			

Note: significant differences are shown in bold. Avg. = averaged, Calc. = calculated, Ind. = individual, MonoE = virtual monoenergetic imaging at 40 keV, PolyE = Polyenergetic imaging, Std = standard, W/L = width/level.

Table 3

Subjective image quality.

Pulmonary artery	Std.-W/L	Ind.-W/L	Calc.-W/L	Avg.-W/L	Std.-W/L vs Ind.-W/L	Ind.-W/L vs Calc.-W/L	Calc.-W/L vs Avg.-W/L
PolyE							
Delineation	1.8 ± 0.5	2.2 ± 0.6	2.1 ± 0.5	2.1 ± 0.5	**<.001**	>.99	>.99
Noise	1.3 ± 0.3	1.7 ± 0.5	1.8 ± 0.4	1.9 ± 0.2	**<.001**	>.99	>.99
MonoE							
Delineation	1.0 ± 0.1	3.6 ± 0.4	3.6 ± 0.4	3.6 ± 0.4	**<.001**	>.99	.99
Noise	2.8 ± 0.4	3.6 ± 0.4	3.6 ± 0.4	3.6 ± 0.3	**<.001**	>.99	>.99

Note: significant differences are shown in bold. Avg. = averaged, Calc. = calculated, Ind. = individual, MonoE = virtual monoenergetic imaging at 40 keV, PolyE = Polyenergetic imaging, Std = standard, W/L = width/level.

In line with previous studies,[18,26–31] we found a strong increase in contrast enhancement in MonoE 40 keV reconstructions, enabling potential image quality improvements, particularly because of the fact, that image noise is not significantly increased in these low energetic, high attenuation MonoE images. Consequently, we found significantly higher CNR values for low keV MonoE images than for the corresponding PolyE reconstructions. This was also observed in former studies of DLCT examinations[14] and is a specific advantage compared to tube-based dual energy systems.[1] However, as proven for other contrast phases and body regions[17,20,21] as well as for different dual-energy techniques,[18,19] major adjustments of the used window settings are needed for MonoE 40 keV images (usually implying substantially higher W and L values in comparison to standard settings), as they inherit great differences in image properties.

Emphasizing these previous findings, our study for pulmonary angiogram DLCT examinations showed a significant difference between the individually adjusted W/L settings (Ind.) for MonoE 40 keV as well as for PolyE and the widely used standard window settings for pulmonary artery assessment. If these individually adjusted window settings were used, significantly higher subjective image quality scores were achieved for both assessment focuses in both reconstruction types compared to the standard window settings.

Table 4

Comparison of subjective image quality ratings between readers (*P* values).

Pulmonary arteries	Std.-W/L	Ind.-W/L	Calc.-W/L	Avg.-W/L
PolyE				
Delineation	.36	.12	.26	.40
Noise	.08	.81	>.99	>.99
MonoE				
Delineation	>.99	.09	.27	.12
Noise	.06	.33	.29	.29

Note: no significant differences were found. Avg. = averaged, Calc. = calculated, Ind. = individual, MonoE = virtual monoenergetic imaging at 40 keV, PolyE = Polyenergetic imaging, Std = standard, W/L = width/level.

Table 5

Measurements of the (left) main pulmonary artery diameter.

PolyE	Diameter, mm (left main pulmonary artery)
Std.-W/L	8.8 ± 2.2
Ind.-W/L	8.6 ± 2.1
Calc.-W/L	8.5 ± 2.2
Avg.-W/L	8.5 ± 2.2
MonoE	
Std.-W/L	12.0 ± 4.1
Ind.-W/L	8.2 ± 2.2
Calc.-W/L	8.2 ± 2.2
Avg.-W/L	8.3 ± 2.2
Comparisons	
Std.-W/L PolyE vs Ind.-W/L PolyE	.33
Ind.-W/L PolyE vs Calc.-W/L PolyE	.27
Calc.-W/L PolyE vs Avg.-W/L PolyE	.99
Std.-W/L MonoE vs Ind.-W/L MonoE	**<.001**
Ind.-W/L MonoE vs Calc.-W/L MonoE	>.99
Calc.-W/L MonoE vs Avg.-W/L MonoE	.48
Ind.-W/L PolyE vs Ind-W/L MonoE	**<.001**

Note: significant differences are shown in bold. Avg. = averaged, Calc. = calculated, Ind. = individual, MonoE = virtual monoenergetic imaging at 40 keV, PolyE = Polyenergetic imaging, Std = standard, W/L = width/level.

Based on regression equations from the different manually adjusted window settings of 50 different examinations, mathematically optimized W/L settings were determined (Calc.) without significant differences to the values of the manual approach. Recent data[19,21] for abdominal CT examinations proposed that for low keV MonoE images W and L values need to be >2 times greater (~2.15× and ~2.47×, respectively) than the corresponding PolyE settings. This is a good correlation to our results of a needed ~2.12× increase in 40 keV MonoE images of the DLCT system. Our results of a ~1.9× increase in W values and a ~0.45× reduction in L values of the overall pulmonary artery attenuation are also concordant with the results of another recently published CTPA study, which showed that W values must be slightly <2 times greater (~×1.6) than the overall pulmonary artery attenuation at 40keV, whereas L values must be approximatively half of the overall pulmonary artery attenuation at 40 keV.[22]

In addition, averaged optimized window settings (Avg.), which were 1020/170 HU [PolyE] and 2070/480 HU [MonoE]), were calculated. Regarding subjective image quality, Calc. and Avg. W/L settings achieved just slightly, but not significantly, lower scores than the Ind. W/L settings and therefore still offered comparable results.

Additionally, a systematic overestimation of vessel diameters was observed if standard window settings were used for MonoE 40 keV images, most likely because of the strong attenuation increase. However, when using individual adjusted window values, the measured vessel diameters were actually slightly smaller in Mono E 40 keV than in PolyE. Similar results were found in a previous study which focused on the assessment of abdominal arteries in MonoE 40 keV images of angiographic phase DLCT examinations.[20] This is probably because of improved capabilities to separate the true vessel lumen from the vessel wall in MonoE 40 keV images. Therefore, standard window settings for MonoE 40 keV images from a DLCT are obsolete for the evaluation of pulmonary arteries, and the use of appropriate values might enable the assessment of the true lumen better than in conventional PolyE images.

To ensure best assessment capabilities, individual adjustment of W and L for low keV MonoE images has to be recommended. However, the manual adjustment of appropriate window values, which allows the evaluation all key image information adequately, is potentially time-consuming. Also, unexperienced readers might struggle with this task as these values most often substantially differ from standard W/L settings. Therefore, we suggest the mathematical approach to derive W/L settings relying on absolute attenuation values of reference regions used in this study. Therefore, an implementation of a (semi-)automatic adjustment of appropriate W/L settings that depends on the reconstruction method used in this study and contrasts situations into viewer systems would be highly desirable for further time saving.

5. Conclusions

Appropriate W/L settings are required for PolyE and MonoE reconstructions of DLCT pulmonary angiogram examinations. The best subjective image quality is offered by individually adjusted window settings; however, these adjustments are potentially time-consuming. Predefined W/L settings for the evaluation of pulmonary arteries of 1020/170 HU (PolyE) and 2070/480 HU (MonoE 40 keV) can be recommended.

Acknowledgments

The authors thank Jordi Garcia-Diaz for assistance with comments that greatly improved the manuscript.

Author contributions

Conceptualization: Andra-Iza Iuga, Jonas Doerner, Stefan Haneder, Jonathan Byrtus, Julian Alexander Luetkens, Tilman Hickethier.
Data curation: Andra-Iza Iuga.
Formal analysis: Andra-Iza Iuga, Stefan Haneder, Tilman Hickethier.
Investigation: Andra-Iza Iuga, Florian Siedek.
Methodology: Andra-Iza Iuga.
Project administration: Andra-Iza Iuga, Tilman Hickethier.
Software: Jonas Doerner, Tilman Hickethier.
Supervision: Andra-Iza Iuga, Jonas Doerner, Julian Alexander Luetkens, David Maintz.
Validation: Andra-Iza Iuga, Florian Siedek, Tilman Hickethier.
Visualization: Tilman Hickethier.
Writing – original draft: Andra-Iza Iuga.
Writing – review & editing: Jonas Doerner, Florian Siedek, Stefan Haneder, Jonathan Byrtus, Julian Alexander Luetkens, David Maintz, Tilman Hickethier.

References

[1] Albrecht MH, Trommer J, Wichmann JL, et al. Comprehensive comparison of virtual monoenergetic and linearly blended reconstruction techniques in third-generation dual-source dual-energy computed tomography angiography of the thorax and abdomen. Invest Radiol 2016;51:582–90.
[2] Gupta S, Wagner-Bartak N, Jensen CT, et al. Dual-energy CT of pancreatic adenocarcinoma: reproducibility of primary tumor measurements and assessment of tumor conspicuity and margin sharpness. Abdom Radiol 2016;41:1317–24.
[3] Weiss J, Notohamiprodjo M, Bongers M, et al. Effect of noise-optimized monoenergetic postprocessing on diagnostic accuracy for detecting incidental pulmonary embolism in portal-venous phase dual-energy computed tomography. Invest Radiol 2017;52:142–7.
[4] Lago KN, Vallejos J, Capuñay C, et al. Dual-energy computed tomography for the detection of focal liver lesions. Radiologia 2017;59:306–12.
[5] Neuhaus V, Abdullayev N, Große Hokamp N, et al. Improvement of image quality in unenhanced dual-layer CT of the head using virtual monoenergetic images compared with polyenergetic single-energy CT. Invest Radiol 2017;52:470–6.
[6] Forghani R, Kelly H, Yu E, et al. Low-energy virtual monochromatic dual-energy computed tomography images for the evaluation of head and neck squamous cell carcinoma: a study of tumor visibility compared with single-energy computed tomography and user acceptance. J Comput Assist Tomogr 2017;41:565–71.
[7] May MS, Bruegel J, Brand M, et al. Computed tomography of the head and neck region for tumor staging-comparison of dual-source, dual-energy and low-kilovolt, single-energy acquisitions. Invest Radiol 2017;52:522–8.
[8] Silva AC, Morse BG, Hara AK, et al. Dual-energy (spectral) CT: applications in abdominal imaging. RadioGraphics 2011;31:
[9] McCollough CH, Leng S, Yu L, et al. Dual- and multi-energy ct: principles, technical approaches, and clinical applications. Radiology 2015;276:637–53.
[10] Dilmanian FA, Wu XY, Parsons EC, et al. Single- and dual-energy CT with monochromatic synchrotron x-rays. Phys Med Biol 1997;42:371–87.
[11] Sellerer T, Noël PB, Patino M, et al. Dual-energy CT: a phantom comparison of different platforms for abdominal imaging. Eur Radiol 2018;28:2745–55.
[12] Yu L, Leng S, McCollough CH. Dual-energy CT-based monochromatic imaging. AJR Am J Roentgenol 2012;1999:S9–15.

[13] Meier A, Wurnig M, Desbiolles L, et al. Advanced virtual monoenergetic images: improving the contrast of dual-energy CT pulmonary angiography. Clin Radiol 2015;70:1244–51.
[14] Doerner J, Hauger M, Hickethier T, et al. Image quality evaluation of dual-layer spectral detector CT of the chest and comparison with conventional CT imaging. Eur J Radiol 2017;93:52–8.
[15] Apfaltrer P, Sudarski S, Schneider D, et al. Value of monoenergetic low-kV dual energy CT datasets for improved image quality of CT pulmonary angiography. Eur J Radiol 2014;83:322–8.
[16] Saba L, Mallarini G. Window settings for the study of calcified carotid plaques with multidetector CT angiography. Am J Neuroradiol 2009;30:1445–50.
[17] Caruso D, Parinella AH, Schoepf UJ, et al. Optimization of window settings for standard and advanced virtual monoenergetic imaging in abdominal dual-energy CT angiography. Abdom Radiol 2017;42: 772–80.
[18] Altenbernd J, Forsting M, Lauenstein T, et al. Improved image quality and detectability of hypovascular liver metastases on dect with different adjusted window settings. Rofo 2017;189:228–32.
[19] De Cecco CN, Caruso D, Schoepf UJ, et al. Optimization of window settings for virtual monoenergetic imaging in dual-energy CT of the liver: A multi-reader evaluation of standard monoenergetic and advanced imaged-based monoenergetic datasets. Eur J Radiol 2016;85:695–9.
[20] Doerner J, Luetkens JA, Iuga A-I, et al. Poly-energetic and virtual mono-energetic images from a novel dual-layer spectral detector CT: optimization of window settings is crucial to improve subjective image quality in abdominal CT angiographies. Abdom Radiol 2018;43:742–50.
[21] Hickethier T, Iuga A-I, Lennartz S, et al. Virtual monoenergetic images from a novel dual-layer spectral detector computed tomography scanner in portal venous phase: adjusted window settings depending on assessment focus are essential for image interpretation. J Comput Assist Tomogr 2018;42:350–6.
[22] D'Angelo T, Bucher AM, Lenga L, et al. Optimisation of window settings for traditional and noise-optimised virtual monoenergetic imaging in dual-energy computed tomography pulmonary angiography. Eur Radiol 2018;28:1393–401.
[23] Hutchinson BD, Navin P, Marom EM, et al. Overdiagnosis of pulmonary embolism by pulmonary CT angiography. Am J Roentgenol 2015;205:271–7.
[24] Wittram C. How I do it: CT pulmonary angiography. Am J Roentgenol 2007;188:1255–61.
[25] Wittram C, Maher MM, Yoo AJ, et al. CT angiography of pulmonary embolism: diagnostic criteria and causes of misdiagnosis. RadioGraphics 2004;24:1219–38.
[26] Schabel C, Bongers M, Sedlmair M, et al. Assessment of the hepatic veins in poor contrast conditions using dual energy CT: evaluation of a novel monoenergetic extrapolation software algorithm. Rofo 2014;186:591–7.
[27] Martin SS, Pfeifer S, Wichmann JL, et al. Noise-optimized virtual monoenergetic dual-energy computed tomography: optimization of kiloelectron volt settings in patients with gastrointestinal stromal tumors. Abdom Radiol 2017;42:718–26.
[28] Martin SS, Albrecht MH, Wichmann JL, et al. Value of a noise-optimized virtual monoenergetic reconstruction technique in dual-energy CT for planning of transcatheter aortic valve replacement. Eur Radiol 2017;27:705–14.
[29] Riffel P, Haubenreisser H, Meyer M, et al. Carotid dual-energy CT angiography: evaluation of low keV calculated monoenergetic datasets by means of a frequency-split approach for noise reduction at low keV levels. Eur J Radiol 2016;85:720–5.
[30] Frellesen C, Fessler F, Hardie AD, et al. Dual-energy CT of the pancreas: Improved carcinoma-to-pancreas contrast with a noise-optimized monoenergetic reconstruction algorithm. Eur J Radiol 2015;84:2052–8.
[31] Albrecht MH, Scholtz JE, Kraft J, et al. Assessment of an advanced monoenergetic reconstruction technique in dual-energy computed tomography of head and neck cancer. Eur Radiol 2015;25:2493–501.